

Unleashing Degradation-Carrying Features in Symmetric U-Net: Simpler and Stronger Baselines for All-in-One Image Restoration

Wenlong Jiao¹, Heyang Lee², Ping Wang¹, Pengfei Zhu³, Qinghua Hu³, Dongwei Ren^{3*}

¹School of Mathematics, Tianjin University

²School of Cybersecurity, Tianjin University

³School of Artificial Intelligence, Tianjin University

{wenlong, chlhy, wang_ping, zhupengfei, huqinghua, rendw}@tju.edu.cn

Abstract

All-in-one image restoration aims to handle diverse degradations (e.g., noise, blur, adverse weather) within a unified framework, yet existing methods increasingly rely on complex architectures (e.g., Mixture-of-Experts, diffusion models) and elaborate degradation prompt strategies. In this work, we reveal a critical insight: well-crafted feature extraction inherently encodes degradation-carrying information, and a symmetric U-Net architecture is sufficient to unleash these cues effectively. By aligning feature scales across encoder-decoder and enabling streamlined cross-scale propagation, our symmetric design preserves intrinsic degradation signals robustly, rendering simple additive fusion in skip connections sufficient for state-of-the-art performance. Our primary baseline, SymUNet, is built on this symmetric U-Net and achieves better results across benchmark datasets than existing approaches while reducing computational cost. We further propose a semantic enhanced variant, SE-SymUNet, which integrates direct semantic injection from frozen CLIP features via simple cross-attention to explicitly amplify degradation priors. Extensive experiments on several benchmarks validate the superiority of our methods. Both baselines SymUNet and SE-SymUNet establish simpler and stronger foundations for future advancements in all-in-one image restoration. The source code is available at <https://github.com/WenlongJiao/SymUNet>.

1. Introduction

All-in-one image restoration aims to recover high-quality images from input images degraded by multiple factors, such as noise, haze, rain, blur and low-light conditions, using a single model. This paradigm offers significant advantages in real-world applications [12, 16, 32], including autonomous driving, surveillance systems and mobile photography, where

*Corresponding author

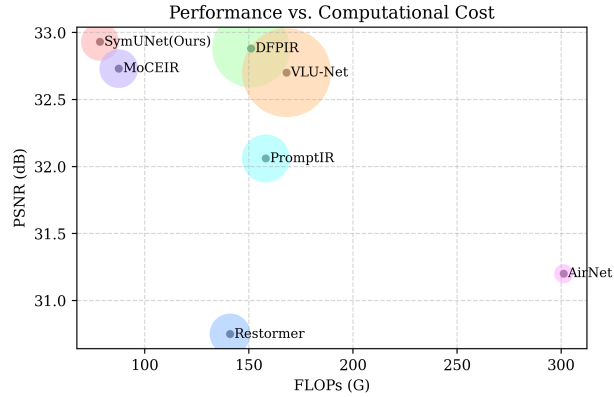


Figure 1. PSNR vs. FLOPs on the three-task benchmark in Table 1. The bubble size corresponds to the total number of parameters. Our SymUNet has fewer parameters than all competing methods, with the sole exception of AirNet. In terms of performance, SymUNet resides in the optimal top-left quadrant (i.e., representing an optimal efficiency-performance balance), thus achieving state-of-the-art results while featuring substantially lower computational overhead.

diverse and often composite degradations should be handled efficiently without task-specific architectures.

Despite significant progress, recent all-in-one methods have drifted toward increasing complexity, as shown in Fig. 1. Prompt-based models [1, 13, 14, 18, 21, 28, 29, 37] rely on multimodal cues to condition degradation-specific behavior. Mixture-of-Experts (MoE) architectures [19, 38, 40, 44] deploy specialized sub-networks for distinct degradation types. Diffusion-based frameworks [1, 19, 21, 24] leverage generative priors for generalization. Recently, agent-based systems [4, 46] use vision-language models (VLMs) to infer and adapt to degradation types dynamically. While these approaches push performance boundaries, their intricate designs (e.g., dynamic routing, large pretrained backbones) inflate computational cost and hinder deployment. More-

over, external priors and complex fusion mechanisms often disturb rather than harness the intrinsic degradation cues already present in the features extracted from degraded images.

In this work, we suggest that well-designed encoder feature extraction inherently embeds degradation-specific information, enabling effective restoration without external complexities. However, common baselines employing asymmetric U-Net architectures, e.g., those derived from Transformer-based models like Restormer [42], perform well in single-task restoration but fail in all-in-one scenarios. Semantic hierarchy misalignment is the main reason, where the encoder captures multi-level features from low-level degradation details to high-level semantics, but asymmetric designs dilute these cues in the heavier decoder. Moreover, due to multi-degradation interference, conflicting signals from heterogeneous degradations clash in unaligned feature spaces, leading to training instabilities that are mitigated in single-task settings by degradation consistency, but are amplified in all-in-one contexts, resulting in inferior generalization across different tasks.

To address these challenges, we suggest a return to simplicity: a symmetric U-Net architecture that aligns feature scales and streamlines cross-scale propagation. This symmetry ensures that degradation-aware features from encoder are preserved without dilution in decoder, rendering simple additive fusion in skip connections sufficient for superior performance. Motivated by this insight, we introduce two strong baselines, SymUNet and SE-SymUNet, for all-in-one image restoration. SymUNet is a standard symmetric U-Net that unleashes degradation-aware features through strict encoder-decoder hierarchy alignment, achieving better performance with fewer parameters. SE-SymUNet is a semantic-enhanced extension that integrates simple cross-attention with frozen CLIP features to inject high-level degradation priors. SE-SymUNet yields modest yet consistent gains, validating the robustness of our symmetric core while avoiding the complexity of full VLM integration.

Extensive evaluations on three-task (denoising, dehazing, deraining) and five-task (denoising, dehazing, deraining, deblurring, low-light enhancement) benchmarks show that SymUNet sets new state-of-the-art performance, outperforming complex competitors with reduced computational cost. SE-SymUNet delivers modest yet consistent further gains, validating the effectiveness of both our core symmetric design and simple semantic integration. In addition, both SymUNet and SE-SymUNet are highly versatile and can be easily extended with advanced modules to make further performance improvements. The contributions of this work can be summarized as:

- We reveal that asymmetric architectures are the core bottleneck for preserving degradation cues, driving a paradigm shift toward simple designs for all-in-one image restoration,

without complex prompts, dynamic routing, or generative priors.

- We propose two strong baselines SymUNet and SE-SymUNet that are easier to extend and more computationally feasible than alternatives, filling a critical gap in the field.
- We conduct extensive experiments and analysis, which enable superior performance on benchmarks and provide insights for future all-in-one restoration architecture development.

2. Related Work

2.1. Task-Specific Image Restoration

Traditional image restoration networks were typically designed for individual tasks, such as denoising [17, 30], dehazing [3, 31], or deraining [8, 36], and each task required a distinct network architecture. Although these models achieved strong results on their respective tasks, deploying multiple networks for different degradations is inefficient and limits practical applicability. Later, unified architectures [6, 10, 11, 34, 41, 42] enabled a single network to handle multiple restoration tasks without redesigning the architecture for each one. Many of these multi-task networks, such as Restormer [42], adopt skip connections using feature concatenation to preserve detailed encoder features. Although these models perform well on individual tasks, their performance often degrades in multi-task scenarios due to large differences in data distributions and conflicts between tasks. Such conflicts increase the complexity of feature representations, making it harder for the network to converge and learn effective restoration mappings across diverse degradations. Consequently, both early single-task networks and later unified models struggle to generalize effectively when faced with heterogeneous or composite degradations, motivating the development of all-in-one image restoration approaches that can efficiently handle multiple degradations within a single framework.

2.2. All-in-One Image Restoration

Early all-in-one image restoration work, such as AirNet [16], introduced unified CNN-based architectures and leveraged contrastive learning to distinguish degradation types in feature space. More recent approaches explore prompt-based modalities [1, 20, 21, 24], where the restoration network is conditioned on additional task-specific information. In this framework, visual prompts encode degradation-specific cues through learnable tokens [23, 28, 35], while textual or multimodal prompts provide guidance via language or combined visual-language instructions [22, 33, 37, 45]. Later studies further incorporate pretrained model priors to offer high-level semantic or structural guidance, enhancing generalization [5, 9, 13, 25, 38]. Other approaches include

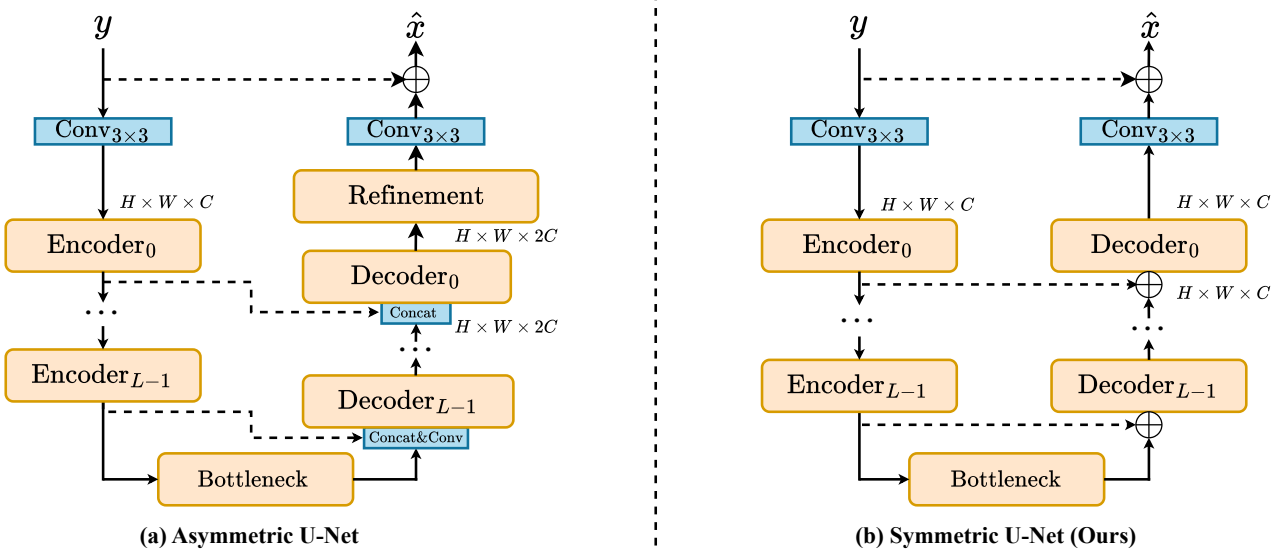


Figure 2. An overview of the architectural philosophies under comparison. **(a) The Asymmetric U-Net** represents a “decoder-heavy” design that is commonly adopted in Restormer [42], PromptIR [28], DFPIR [32], etc. It employs concatenation-based skip connections, which causes an abrupt channel expansion (e.g., from C to $2C$) in the decoder, and appends auxiliary refinement blocks. This asymmetric hierarchy creates a complex and indirect path for feature fusion. **(b) Our Symmetric U-Net (SymUNet)** is built on the strict U-shape architecture, where the feature extraction blocks in encoder, decoder and bottleneck share the same structure. SymUNet uses simple additive skip connections to maintain consistent channel dimensions and ensure a direct and efficient flow of degradation-aware information from encoder to decoder.

Mixture-of-Experts (MoE) frameworks [40, 44], which allocate specialized branches for different degradations, and agent-based systems [4, 46], where vision-language agents reason about degradation types and guide adaptive restoration strategies. Although these methods improve generalization and adaptability, they rely heavily on external prior knowledge, which can obscure intrinsic degradation features and impede the network from fully learning effective restoration capabilities. In contrast, a well-designed Transformer backbone [6, 42] can capture both global dependencies and local structures without auxiliary priors, focusing directly on the information present in the degraded image itself. Motivated by this, we propose a simple Transformer baseline that achieves efficient and effective all-in-one restoration by focusing purely on essential visual information.

3. Proposed Method

Our methodology introduces two distinct models for all-in-one image restoration. We first present **SymUNet**, our baseline restoration network, built upon a symmetric U-shape architecture with a simple yet effective fusion strategy. Building upon this, we then introduce **SE-SymUNet**, which enhances this strong baseline by incorporating a bidirectional semantic guidance module that leverages frozen CLIP features.

3.1. Motivation

In all-in-one image restoration, where a single model must handle diverse and unknown degradations, the U-Net architecture is a common foundation. However, a prevalent design pattern in leading models is a subtle yet impactful form of architectural asymmetry, as shown in Fig. 2(a). This is often manifested in two ways: *(i)* the channel dimension doubles in the final decoder stage after concatenating features from the skip connection, and *(ii)* additional “refinement blocks” are appended after the main decoder. These choices create a significantly heavier decoder, operating on the assumption that a more complex reconstruction module is necessary to tackle varied degradations.

We challenge this “decoder-heavy” design philosophy. For the all-in-one task, the encoder must extract crucial and degradation-aware cues from the input images. We suggest that the aforementioned asymmetry disrupts the effective use of these cues. The abrupt channel expansion in the decoder forces the network to learn a complex transformation from the skip connection’s compact features, while auxiliary refinement blocks process features that have already lost the direct and fine-grained guidance from the deepest encoder layers. This can lead to inefficient feature fusion and a diluted flow of degradation-specific information. We suggest that this added complexity is often unnecessary, since a streamlined encoder is fully capable of isolating these degra-

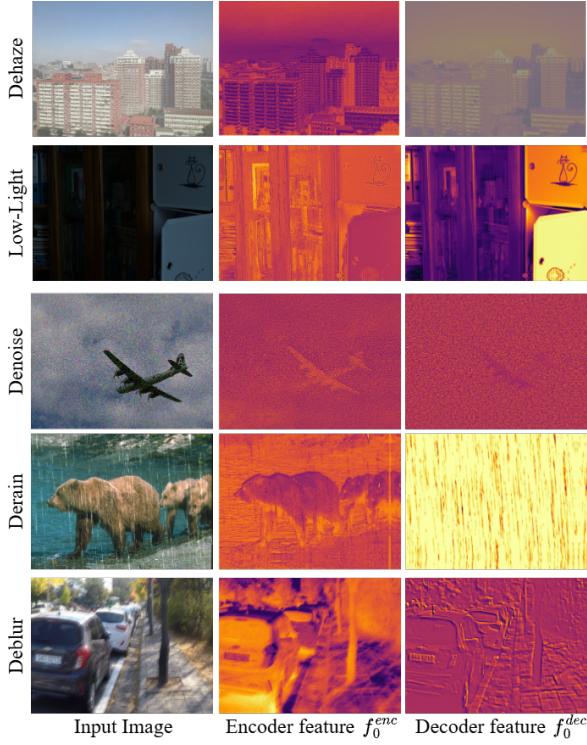


Figure 3. Visualization of degradation-carrying features learned by our SymUNet. This figure supports our motivation: a streamlined and symmetric architecture is highly effective at extracting and modeling diverse degradation-aware information. For each task, the decoder feature f_0^{enc} actually carries degradation information, and can be well propagated to the decoder feature f_0^{dec} , which isolates the specific degradation pattern, such as atmospheric haze, light condition, random noise structure, directional rain streaks and blur boundaries. This demonstrates that architectural simplicity provides a powerful and sufficient foundation for the complex demands of all-in-one restoration.

dation patterns, a phenomenon we visually validate with the learned residual features in Fig. 3.

In contrast, we propose that standard architectural symmetry is a more effective and efficient principle. By maintaining consistent channel dimensions across corresponding encoder-decoder stages and forgoing auxiliary blocks, we create a balanced and direct information pathway. This design ensures that degradation cues from the encoder are seamlessly fused and preserved with high fidelity throughout the network. Our symmetric U-Net is built on this principle, demonstrating that a streamlined and balanced architecture is inherently more powerful for the complex demands of all-in-one restoration.

3.2. Primary Baseline: SymUNet

In contrast to recent trends towards complex and asymmetric architectures, our baseline, SymUNet, deliberately returns to a simple, symmetric, and efficient U-shape design. We posit

that this streamlined structure is inherently more robust for the all-in-one restoration task.

Our baseline is built on a U-shape architecture with L scales, comprising L encoder layers, L decoder layers, and a bottleneck layer, as illustrated in Fig. 2(b). The network begins with an initial convolutional layer that maps the input degraded image $\mathbf{y} \in \mathbb{R}^{H \times W \times C_{in}}$ to a higher-dimensional feature space $\mathbf{f}_0^{enc} \in \mathbb{R}^{H \times W \times C}$. Each layer of the encoder, decoder, and bottleneck consists of multiple feature extraction blocks, which share the same structure and are adapted from the efficient Transformer block design in Restormer [42]. The network concludes with a final convolutional layer that converts features from the last decoder layer into a residual image, which is added to the input to obtain the final restored image $\hat{\mathbf{x}} \in \mathbb{R}^{H \times W \times C_{in}}$.

The overall pipeline is as follows:

$$\begin{aligned}
 \mathbf{f}_0^{enc} &= \text{Conv}_{3 \times 3}(\mathbf{y}), \\
 \mathbf{s}_i &= \text{Encoder}_i(\mathbf{f}_0^{enc}), \quad i \in \{0, \dots, L-1\} \\
 \mathbf{f}_{i+1}^{enc} &= \text{DOWN}_{i+1}(\mathbf{s}_i), \quad i \in \{0, \dots, L-1\} \\
 \mathbf{f}_L^{dec} &= \text{Bottleneck}(\mathbf{f}_L^{enc}), \\
 \mathbf{f}_{in}^{(i)} &= \text{UP}_{i+1}(\mathbf{f}_{i+1}^{dec}) + \mathbf{s}_i, \quad i \in \{L-1, \dots, 0\} \\
 \mathbf{f}_0^{dec} &= \text{Decoder}_i(\mathbf{f}_{in}^{(i)}), \quad i \in \{L-1, \dots, 0\} \\
 \hat{\mathbf{x}} &= \text{Conv}_{3 \times 3}(\mathbf{f}_0^{dec}) + \mathbf{y},
 \end{aligned} \tag{1}$$

where UP and DOWN represent upsampling and downsampling operations.

This structure ensures that the skip connection \mathbf{s}_{i-1} provides the features from the i -th encoder stage before they are downsampled, preserving high-resolution details for the corresponding decoder stage.

Symmetric and Efficient Architecture. The key to our baseline’s strong performance lies in its architectural design, which differs from Restormer [42], PromptIR [28], DFPIR [32] in three crucial aspects: *(i) Symmetric Structure*: Our encoder and decoder are symmetric in terms of block counts, creating a balanced architectural flow. *(ii) Consistent Channel Dimensions*: Unlike asymmetric designs where the channel count doubles after the final skip connection, our decoder maintains a consistent, narrower channel width, forcing the network to learn more compact representations. *(iii) No Auxiliary Refinement Blocks*: Our network’s output is taken directly from the final decoder stage, emphasizing simplicity. We suggest that this combination of design choices provides a stronger inductive bias for the all-in-one restoration task.

3.3. Semantic Enhanced Baseline: SE-SymUNet

Our SE-SymUNet enhances the primary SymUNet baseline by integrating our bidirectional semantic guidance mechanism, as shown in Fig. 4. This is achieved by effectively

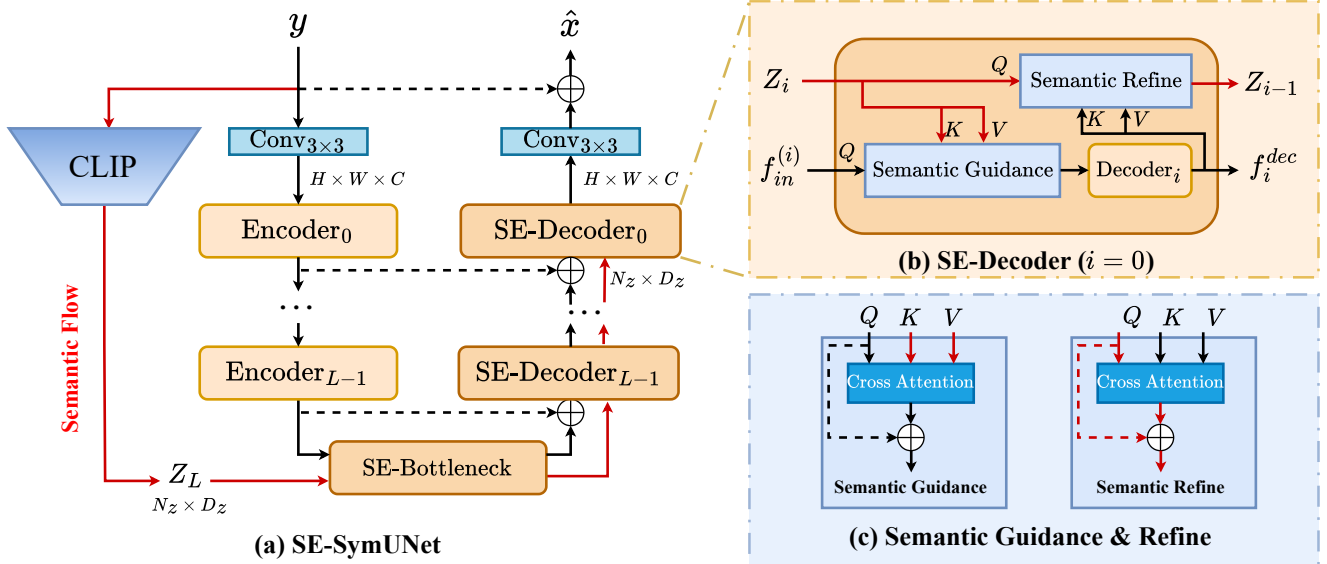


Figure 4. An overview of our semantic enhanced baseline SE-SymUNet, which is built by augmenting SymUNet. In particular, SE-SymUNet introduces a bidirectional semantic guidance module to inject and refine CLIP priors into SymUNet. At each decoder stage, image features f are first refined by the CLIP semantic context Z via Semantic Guidance Module. Subsequently, the semantic context itself is updated by the refined image features f' via Semantic Refinement Module, creating an iterative feedback loop that makes the guidance adaptive. SE-Bottleneck has the same structure with SE-Decoder.

wrapping the standard Bottleneck and Decoder modules to create their semantic-enhanced counterparts, which we term the SE-Bottleneck and SE-Decoder. The feature extraction blocks in SE-Bottleneck and SE-Decoder also share the same structure. These new composite modules create an adaptive feedback loop between image features and high-level semantic context.

Bidirectional Semantic Guidance Module. The core of our enhancement is a module designed to foster a synergistic dialogue between an image feature map f and a semantic context Z . It consists of two complementary operations:

First, the **Semantic Guidance** step infuses semantic priors into the restoration pathway. It allows image features to query the semantic context, enabling each local region to draw upon relevant high-level concepts to guide its reconstruction. The operation is defined as:

$$\text{SemanticGuidance}(f, Z) = f + \text{CA}(f, Z, Z), \quad (2)$$

where CA denotes multi-head cross-attention. To perform this operation, the spatial feature map f is treated as a sequence of patch-based tokens.

Second, the **Semantic Refinement** step updates the semantic context itself, grounding it in the newly clarified visual evidence. The semantic context queries the refined image features to recalibrate its understanding, making it more accurate for subsequent stages. This operation is defined as:

$$\text{SemanticRefine}(f, Z) = Z + \text{CA}(Z, f, f). \quad (3)$$

Semantic Context Extraction. The semantic context Z used in the guidance module is initialized from the input image. We extract an initial context, Z_L , using the frozen Vision Transformer from CLIP (ViT-L/14). By leveraging the `last_hidden_state`, we obtain a sequence of patch-based tokens, $Z_L \in \mathbb{R}^{N_z \times D_z}$ (where $N_z = 257$ and $D_z = 1024$), which retains granular, spatially-aware information. This Z_L serves as the initial state for the semantic context that is then iteratively refined.

Architectural Integration. With the guidance functions defined, we now detail their integration. The encoder architecture remains identical to **SymUNet**. The upward path, from the bottleneck (level L) to the final output (level 0), is defined by the following iterative process.

Starting with the initial context Z_L , for each level i from L down to 0:

$$f_{in}^{(i)} = \begin{cases} f_L^{enc}, & \text{if } i = L \\ \text{UP}_{i+1}(f_{i+1}^{dec}) + s_i, & \text{if } i < L \end{cases} \quad (4)$$

$$f'_{in} = \text{SemanticGuidance}(f_{in}^{(i)}, Z_i), \quad (5)$$

$$f_i^{dec} = \begin{cases} \text{Bottleneck}(f'_{in}), & \text{if } i = L \\ \text{Decoder}_i(f'_{in}), & \text{if } i < L \end{cases} \quad (6)$$

$$Z_{i-1} = \text{SemanticRefine}(f_i^{dec}, Z_i). \quad (7)$$

This iterative cycle ensures that as the image features become cleaner, the semantic guidance in the next stage becomes

correspondingly more precise. The final output is generated identically to the baseline $\hat{\mathbf{x}} = \text{Conv}_{3 \times 3}(\mathbf{f}_0^{dec}) + \mathbf{y}$.

4. Experiments

4.1. Datasets

We evaluate our models on two all-in-one (multi-task) restoration scenarios: a three-task setting and a more challenging five-task setting.

Three-Task All-in-One Restoration. This task involves simultaneously training a single model for Denoising, Dehazing, and Deraining. For training, we construct a large-scale dataset by combining several task-specific benchmarks. This includes 400 general-purpose images from BSD400 [2], 4,744 images from WED [26], 72,135 hazy images from the RESIDE- β -OTS [15] training set, and 200 rainy images from Rain100L [39]. This results in a combined training set of 77,479 images. For evaluation, we use standard benchmarks for each task: CBSD68 [2] (68 images) for denoising, SOTS-Outdoor [15] (500 images) for dehazing, and the test set of Rain100L [39] (100 images) for deraining.

Five-Task All-in-One Restoration. To assess the generalization capability of our models, we expand the scope to five concurrent tasks, adding Deblurring and Low-Light enhancement. To train for this more complex scenario, we augment the previous training set with 2,103 blurry images from the GoPro [27] training set and 485 low-light images from the LOL [7] training set. The final training dataset for this five-task setting contains 80,067 images. Evaluation is performed on the same benchmarks for denoising, dehazing, and deraining, supplemented by the GoPro [27] test set (1,111 images) for deblurring and the LOL [7] test set (15 images) for low-light enhancement.

4.2. Implementation Details

Model Architecture. Both our SymUNet and SE-SymUNet are based on a 4-level U-shape architecture, i.e., $L = 3$. The encoder consists of three stages with 4, 6, and 6 feature extraction blocks, respectively. The bottleneck layer contains 8 feature extraction blocks. The decoder is structured symmetrically, with its three stages containing 6, 6, and 4 feature extraction blocks. For SE-SymUNet, the semantic context is extracted using the pre-trained CLIP Vision Transformer (ViT-L/14). During the direct semantic injection process, the patch size (p) used to partition the image feature maps is set to 2 for the bottleneck layer, and 4 for all three decoder layers.

Training Details. Our models were implemented using PyTorch and trained on NVIDIA RTX 5880 Ada Generation GPUs. We used the AdamW optimizer with an initial

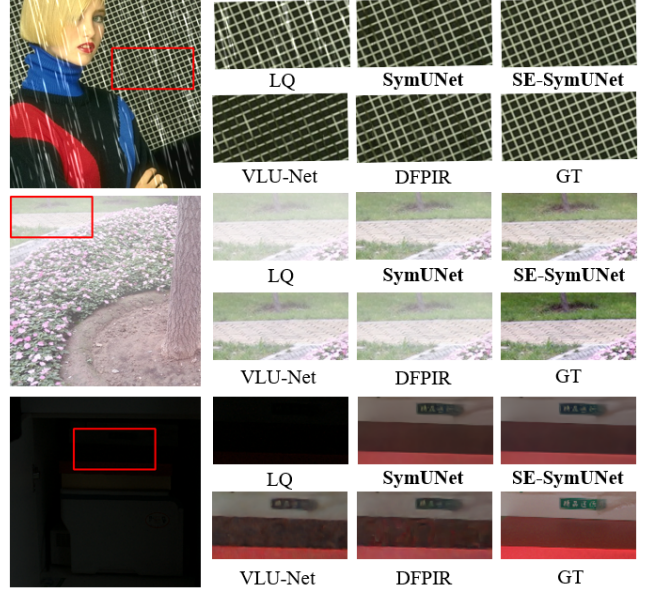


Figure 5. Visual comparison of our methods against state-of-the-art methods on the five-task all-in-one benchmark. From top to bottom, the examples showcase results for deraining, dehazing, and low-light enhancement. Our methods, particularly SE-SymUNet, outperform at removing complex degradations while preserving fine textures (first row), restoring natural color and contrast from dense haze (second row), and recovering fine details with fewer color artifacts in extreme low-light conditions (third row). These results highlight the superior visual quality and robustness of our proposed architectures.

learning rate of 1×10^{-3} , parameters $\beta_1 = 0.9$, $\beta_2 = 0.999$, and a weight decay of 1×10^{-3} . A cosine annealing schedule was used to decay the learning rate to a minimum of 1×10^{-7} . Our loss function is $\mathcal{L}_{\text{total}} = \mathcal{L}_1 + \lambda \mathcal{L}_{\text{FFT}}$, where \mathcal{L}_1 is the standard L1 pixel loss between the predicted image $\hat{\mathbf{x}}$ and the ground-truth \mathbf{x} , and the frequency-domain loss is $\mathcal{L}_{\text{FFT}} = \|\mathcal{F}(\hat{\mathbf{x}}) - \mathcal{F}(\mathbf{x})\|_1$. Here, \mathcal{F} denotes the 2D Fast Fourier Transform operator, and we set the weighting coefficient $\lambda = 0.1$. The three-task model was trained for 300,000 iterations, while the five-task model was trained for 400,000 iterations. We used a batch size of 32, with random 128×128 crops and standard augmentations (random flips).

4.3. Main Results

We present the quantitative results of our models against state-of-the-art all-in-one image restoration methods in Table 1 and Table 2. The evaluation across both benchmarks demonstrates the effectiveness of our proposed models, with our symmetric U-Net design establishing a new state-of-the-art performance baseline.

Table 1. Quantitative comparison for the three-task all-in-one restoration benchmark. We report PSNR (dB) / SSIM. Best and second-best results are highlighted in **bold** and underline, respectively. * Results are cited from [12], as these methods were not originally designed for the all-in-one restoration task.

Method	Dehazing	Deraining Rain100L	Denoising on BSD68			Average
	SOTS-Outdoor		$\sigma = 15$	$\sigma = 25$	$\sigma = 50$	
Restormer* [42]	27.78/0.958	33.78/0.958	33.72/0.865	30.67/0.865	27.63/0.792	30.75/0.901
NAFNet* [6]	24.11/0.960	33.64/0.956	33.18/0.918	30.47/0.865	27.12/0.754	29.67/0.844
AirNet [16]	27.94/0.962	34.90/0.968	33.92/0.933	31.26/0.888	28.00/0.797	31.20/0.910
PromptIR [28]	30.58/0.974	36.37/0.972	33.98/0.933	31.31/0.888	28.06/0.799	32.06/0.913
InstructIR-3D [9]	30.22/0.959	37.98/0.978	34.15/0.933	31.52/0.890	28.30/0.804	32.43/0.913
Perceive-IR [45]	30.87/0.975	38.29/0.980	34.13/0.934	31.53/0.890	28.31/0.804	32.63/0.917
VLU-Net [43]	30.71/0.980	38.93/0.984	34.13/0.935	31.48/0.892	28.23/0.804	32.70/0.919
MoCE-IR [40]	31.34/0.979	38.57/0.984	34.11/0.932	31.45/0.888	28.18/0.800	32.73/0.917
DFPIR [32]	<u>31.87</u> /0.980	38.65/0.982	34.14/0.935	31.47/0.893	28.25/0.806	32.88/0.919
SymUNet (Ours)	<u>31.40/0.981</u>	<u>39.12/0.985</u>	<u>34.22/0.937</u>	<u>31.57/0.894</u>	<u>28.32/0.808</u>	<u>32.93/0.921</u>
SE-SymUNet (Ours)	32.02/0.983	39.23/0.986	34.23/0.937	31.58/0.895	28.33/0.809	33.08/0.922

Table 2. Quantitative comparison for the five-task all-in-one restoration benchmark. We report PSNR (dB) / SSIM. Best and second-best results are highlighted in **bold** and underline, respectively. * Results are cited from the survey paper [12], as the original papers for these methods do not report on this specific all-in-one benchmark.

Method	Dehazing	Deraining Rain100L	Denoising BSD68 ($\sigma = 25$)	Deblurring	Low-Light	Average
	SOTS-Outdoor			GoPro	LOL	
Restormer* [42]	24.09/0.927	34.81/0.960	31.49/0.884	27.22/0.829	20.41/0.806	27.60/0.881
NAFNet* [6]	25.23/0.939	35.56/0.967	31.02/0.883	26.53/0.808	20.49/0.809	27.76/0.881
AirNet* [16]	21.04/0.884	32.98/0.951	30.91/0.882	24.35/0.781	18.18/0.735	25.49/0.846
PromptIR* [28]	26.54/0.949	36.37/0.970	31.47/0.886	28.71/0.881	22.68/0.832	29.15/0.904
InstructIR-5D [9]	27.10/0.956	36.84/0.973	31.40/0.887	29.40/0.886	23.00/0.836	29.55/0.907
Perceive-IR [45]	28.19/0.964	37.25/0.977	<u>31.44/0.887</u>	<u>29.46/0.886</u>	22.88/0.833	29.84/0.909
VLU-Net [43]	30.84/0.980	<u>38.54/0.982</u>	31.43/0.891	27.46/0.840	22.29/0.833	30.11/0.905
MoCE-IR [40]	30.48/0.974	38.04/0.982	31.34/0.887	30.05/0.899	23.00/0.852	30.58/0.919
DFPIR [32]	<u>31.64/0.979</u>	37.62/0.978	31.29/0.889	28.82/0.873	23.82/0.843	<u>30.64/0.913</u>
SymUNet (Ours)	31.31/0.979	38.05/0.981	<u>31.38/0.891</u>	28.12/0.855	<u>23.27/0.858</u>	30.43/0.913
SE-SymUNet (Ours)	32.15/0.982	<u>38.44/0.983</u>	31.45/0.892	28.40/0.864	<u>23.22/0.861</u>	30.73/0.916

4.3.1. Three-Task All-in-One Restoration

The results for the three-task benchmark are presented in Table 1. Our models demonstrate state-of-the-art performance. The baseline SymUNet achieves an average PSNR of 32.93 dB, establishing a new state-of-the-art that surpasses all other listed methods. This result is particularly noteworthy as SymUNet is a standard symmetric U-Net without specialized modules, suggesting that a well-balanced architecture is highly effective for multi-degradation restoration by enabling a more stable and efficient flow of features through its aligned encoder-decoder pathways.

Our semantically-enhanced model, SE-SymUNet, further elevates the average performance to 33.08 dB PSNR and achieves the top PSNR score across all individual tasks. The

most significant gain over our baseline is observed in the dehazing task (+0.62 dB), indicating that explicit semantic guidance is particularly beneficial for resolving spatially extensive degradations where scene context is crucial. This consistent and top-ranking performance confirms the value of our lightweight guidance mechanism, while the exceptional performance of the baseline itself strongly underscores the central importance of a simple and symmetric architectural foundation for this restoration paradigm.

4.3.2. Five-Task All-in-One Restoration

The five-task setting, presented in Table 2, introduces a more significant challenge by adding deblurring and low-light enhancement. In this highly complex scenario, our SE-

Table 3. Ablation on architectural symmetry. We report the average PSNR (dB) and SSIM across all test sets of the three-task benchmark.

Configuration	PSNR	SSIM
(a) Asymmetric Baseline	32.55	0.919
(b) Symmetric Baseline (SymUNet)	32.93	0.921

SymUNet again establishes a new state-of-the-art, achieving the highest average PSNR of 30.73 dB. This result surpasses all other listed methods and demonstrates the strong generalization of our approach when faced with a wider array of degradations. The baseline SymUNet also delivers a highly competitive performance of 30.43 dB, underscoring the robustness of our core symmetric architecture.

A closer look at the per-task results reveals the strengths of our design. Our SE-SymUNet demonstrates dominant performance in Dehazing (+0.51 dB over the second best) and achieves top-tier results in Deraining and Denoising. This suggests our symmetric architecture, augmented with semantic guidance, excels at handling degradations that corrupt fine-grained details and affect local image regions. For tasks such as deblurring and low-light enhancement, our model remains competitive, indicating that the semantic context provided by CLIP offers a valuable prior for addressing a wide spectrum of degradations. The consistent high performance across this diverse five-task benchmark validates that our simple, symmetric design serves as a powerful and effective foundation for complex multi-degradation restoration. This quantitative superiority is consistent with the qualitative results shown in Fig. 5, where our models demonstrate a clear advantage in preserving fine details and restoring faithful colors with fewer visual artifacts.

4.4. Ablation Study

To validate the effectiveness of our key design choices, we conduct a series of ablation studies on the three-task benchmark. For all ablation experiments, we maintain the same training settings as described in Section 4.2 to ensure a fair comparison. The results, summarized in Table 3 and Table 4, systematically demonstrate the contribution of each component.

4.4.1. Impact of Architectural Symmetry

Our central hypothesis is that a simple, symmetric U-Net provides a stronger foundation for all-in-one restoration than the “decoder-heavy” designs prevalent in many state-of-the-art models. To verify this, we construct an (a) Asymmetric Baseline that mimics this design philosophy. Specifically, starting from our SymUNet architecture, we introduce two modifications: 1) the channel dimension in the final decoder stage is doubled after concatenating features from the cor-

Table 4. Ablation on the semantic guidance module. We progressively add components to our strong SymUNet baseline.

Configuration	PSNR	SSIM
(a) Baseline (SymUNet)	32.93	0.921
(b) + Semantic Guidance (one-way)	33.02	0.921
(c) + Bidirectional Guidance (SE-SymUNet)	33.08	0.922

responding skip connection, and 2) a series of refinement blocks are appended after the main decoder output.

As shown in Table 3, our SymUNet, which adheres to the symmetric principle, achieves a superior average PSNR of 32.93 dB. This marks a significant gain of 0.38 dB over the asymmetric configuration (a). This result strongly supports our motivation. The performance degradation in the asymmetric model suggests that a heavier and more complex decoder can disrupt the direct and efficient flow of degradation-aware information from the encoder. In contrast, our streamlined and symmetric architecture ensures a more effective fusion of features, validating it as a more powerful and principled choice for all-in-one restoration.

4.4.2. Contribution of Semantic Guidance

Having established the superiority of our symmetric baseline, we next evaluate the impact of our semantic guidance module by progressively adding its components to SymUNet. As shown in Table 4, incorporating the unidirectional ‘Semantic Guidance’ mechanism (b) notably improves the average PSNR over the baseline. Subsequently, enabling the full bidirectional feedback loop with ‘Semantic Refine’ (c), which constitutes our full SE-SymUNet, further boosts the performance to the highest level. This step-by-step improvement validates our bidirectional approach and demonstrates its tangible benefit over one-way injection. More importantly, it highlights that even a straightforward guidance mechanism, implemented with cross-attention, can effectively harness high-level semantic priors to unlock a significant gain in restoration performance.

5. Conclusion

In this work, we have demonstrated that symmetric U-Net architectures effectively unleash inherent degradation-carrying features for all-in-one image restoration, outperforming complex models like MoE, diffusion-based, and prompt-conditioned methods. By aligning encoder-decoder hierarchies and employing streamlined skip connections, our SymUNet baseline preserves fine-grained degradation cues without dilution or interference, enabling stable training and superior generalization across heterogeneous degradations. The enhanced SE-SymUNet incorporates bidirectional semantic injection from frozen CLIP priors, yielding modest yet consistent improvements and underscoring the robust-

ness of the symmetric design. Extensive experiments on three-task and five-task benchmarks validate our approach: SymUNet achieves state-of-the-art PSNR and SSIM, surpassing asymmetric baselines like Restormer derivatives with fewer parameters and no auxiliary stabilizers. Future work will extend to video restoration, integrate diffusion priors for composites, optimize for real-time devices, and add multi-modal inputs for enhanced adaptability.

References

- [1] Yuang Ai, Huaibo Huang, Xiaoqiang Zhou, Jieyang Wang, and Ran He. Multimodal prompt receiver: Empower adaptiveness generalizability and fidelity for all-in-one image restoration. In *Proceedings of the IEEE/CVF Conference on Computer Vision and Pattern Recognition*, pages 25432–25444, 2024. [1](#) [2](#)
- [2] Pablo Arbelaez, Michael Maire, Charless Fowlkes, and Jitendra Malik. Contour detection and hierarchical image segmentation. *IEEE transactions on pattern analysis and machine intelligence*, 33(5):898–916, 2010. [6](#)
- [3] Bolun Cai, Xiangmin Xu, Kui Jia, Chunmei Qing, and Dacheng Tao. Dehazenet: An end-to-end system for single image haze removal. *IEEE transactions on image processing*, 25(11):5187–5198, 2016. [2](#)
- [4] Haoyu Chen, Wenbo Li, Jinjin Gu, Jingjing Ren, Sixiang Chen, Tian Ye, Renjing Pei, Kaiwen Zhou, Fenglong Song, and Lei Zhu. Restoreagent: Autonomous image restoration agent via multimodal large language models. *Advances in Neural Information Processing Systems*, 37:110643–110666, 2024. [1](#) [3](#)
- [5] I Chen, Wei-Ting Chen, Yu-Wei Liu, Yuan-Chun Chiang, Sy-Yen Kuo, Ming-Hsuan Yang, et al. Unirestore: Unified perceptual and task-oriented image restoration model using diffusion prior. In *Proceedings of the Computer Vision and Pattern Recognition Conference*, pages 17969–17979, 2025. [2](#)
- [6] Liangyu Chen, Xiaojie Chu, Xiangyu Zhang, and Jian Sun. Simple baselines for image restoration. In *European conference on computer vision*, pages 17–33. Springer, 2022. [2](#) [3](#) [7](#)
- [7] Wei Chen, Wenjing Wang, Wenhan Yang, and Jiaying Liu. Deep retinex decomposition for low-light enhancement. In *British Machine Vision Conference*. British Machine Vision Association, 2018. [6](#)
- [8] Xiang Chen, Hao Li, Mingqiang Li, and Jinshan Pan. Learning a sparse transformer network for effective image deraining. In *Proceedings of the IEEE/CVF conference on computer vision and pattern recognition*, pages 5896–5905, 2023. [2](#)
- [9] Marcos V Conde, Gregor Geigle, and Radu Timofte. Instructir: High-quality image restoration following human instructions. In *European Conference on Computer Vision*, pages 1–21. Springer, 2024. [2](#) [7](#)
- [10] Yuning Cui, Wenqi Ren, Xiaochun Cao, and Alois Knoll. Image restoration via frequency selection. *IEEE Transactions on Pattern Analysis and Machine Intelligence*, 46(2):1093–1108, 2023. [2](#)
- [11] Hang Guo, Jinmin Li, Tao Dai, Zhihao Ouyang, Xudong Ren, and Shu-Tao Xia. Mambair: A simple baseline for image restoration with state-space model. In *European conference on computer vision*, pages 222–241. Springer, 2024. [2](#)
- [12] Junjun Jiang, Zengyuan Zuo, Gang Wu, Kui Jiang, and Xianming Liu. A survey on all-in-one image restoration: Taxonomy, evaluation and future trends. *IEEE Transactions on Pattern Analysis and Machine Intelligence*, 2025. [1](#) [7](#)
- [13] Yitong Jiang, Zhaoyang Zhang, Tianfan Xue, and Jinwei Gu. Autodir: Automatic all-in-one image restoration with latent diffusion. In *European Conference on Computer Vision*, pages 340–359. Springer, 2024. [1](#) [2](#)
- [14] Xiangtao Kong, Chao Dong, and Lei Zhang. Towards effective multiple-in-one image restoration: A sequential and prompt learning strategy. *arXiv preprint arXiv:2401.03379*, 2024. [1](#)
- [15] Boyi Li, Wenqi Ren, Dengpan Fu, Dacheng Tao, Dan Feng, Wenjun Zeng, and Zhangyang Wang. Benchmarking single-image dehazing and beyond. *IEEE transactions on image processing*, 28(1):492–505, 2018. [6](#)
- [16] Boyun Li, Xiao Liu, Peng Hu, Zhongqin Wu, Jiancheng Lv, and Xi Peng. All-in-one image restoration for unknown corruption. In *Proceedings of the IEEE/CVF conference on computer vision and pattern recognition*, pages 17452–17462, 2022. [1](#) [2](#) [7](#)
- [17] Jingyun Liang, Jiezheng Cao, Guolei Sun, Kai Zhang, Luc Van Gool, and Radu Timofte. Swinir: Image restoration using swin transformer. In *Proceedings of the IEEE/CVF international conference on computer vision*, pages 1833–1844, 2021. [2](#)
- [18] Rongxin Liao, Feng Li, Yanyan Wei, Zenglin Shi, Le Zhang, Huihui Bai, and Meng Wang. Prompt to restore, restore to prompt: Cyclic prompting for universal adverse weather removal. *arXiv preprint arXiv:2503.09013*, 2025. [1](#)
- [19] Jingbo Lin, Zhilu Zhang, Wenbo Li, Renjing Pei, Hang Xu, Hongzhi Zhang, and Wangmeng Zuo. Unirestorer: Universal image restoration via adaptively estimating image degradation at proper granularity. *arXiv preprint arXiv:2412.20157*, 2024. [1](#)
- [20] Jingbo Lin, Zhilu Zhang, Yuxiang Wei, Dongwei Ren, Dongsheng Jiang, Qi Tian, and Wangmeng Zuo. Improving image restoration through removing degradations in textual representations. In *Proceedings of the IEEE/CVF Conference on Computer Vision and Pattern Recognition*, pages 2866–2878, 2024. [2](#)
- [21] Minghao Liu, Wenhan Yang, Jinyi Luo, and Jiaying Liu. Up-restorer: When unrolling meets prompts for unified image restoration. In *Proceedings of the AAAI Conference on Artificial Intelligence*, pages 5513–5522, 2025. [1](#) [2](#)
- [22] Yihao Liu, Xiangyu Chen, Xianzheng Ma, Xintao Wang, Jiantao Zhou, Yu Qiao, and Chao Dong. Unifying image processing as visual prompting question answering. In *International Conference on Machine Learning*, 2024. [2](#)
- [23] Yidi Liu, Dong Li, Xueyang Fu, Xin Lu, Jie Huang, and Zheng-Jun Zha. Uhd-processer: Unified uhd image restoration with progressive frequency learning and degradation-aware prompts. In *Proceedings of the Computer Vision and*

Pattern Recognition Conference, pages 23121–23130, 2025. 2

[24] Wenyang Luo, Haina Qin, Zewen Chen, Libin Wang, Dandan Zheng, Yuming Li, Yufan Liu, Bing Li, and Weiming Hu. Visual-instructed degradation diffusion for all-in-one image restoration. In *Proceedings of the Computer Vision and Pattern Recognition Conference*, pages 12764–12777, 2025. 1, 2

[25] Ziwei Luo, Fredrik K. Gustafsson, Zheng Zhao, Jens Sjölund, and Thomas B. Schön. Controlling vision-language models for multi-task image restoration. In *The Twelfth International Conference on Learning Representations*, 2024. 2

[26] Kede Ma, Zhengfang Duanmu, Qingbo Wu, Zhou Wang, Hongwei Yong, Hongliang Li, and Lei Zhang. Waterloo exploration database: New challenges for image quality assessment models. *IEEE Transactions on Image Processing*, 26(2):1004–1016, 2016. 6

[27] Seungjun Nah, Tae Hyun Kim, and Kyoung Mu Lee. Deep multi-scale convolutional neural network for dynamic scene deblurring. In *Proceedings of the IEEE conference on computer vision and pattern recognition*, pages 3883–3891, 2017. 6

[28] Vaishnav Potlapalli, Syed Waqas Zamir, Salman Khan, and Fahad Khan. Promptir: Prompting for all-in-one image restoration. In *Thirty-seventh Conference on Neural Information Processing Systems*, 2023. 1, 2, 3, 4, 7

[29] Alec Radford, Jong Wook Kim, Chris Hallacy, Aditya Ramesh, Gabriel Goh, Sandhini Agarwal, Girish Sastry, Amanda Askell, Pamela Mishkin, Jack Clark, et al. Learning transferable visual models from natural language supervision. In *International conference on machine learning*, pages 8748–8763. PMLR, 2021. 1

[30] Hao Shen, Zhong-Qiu Zhao, and Wandi Zhang. Adaptive dynamic filtering network for image denoising. In *Proceedings of the AAAI Conference on Artificial Intelligence*, pages 2227–2235, 2023. 2

[31] Yuda Song, Zhuqing He, Hui Qian, and Xin Du. Vision transformers for single image dehazing. *IEEE Transactions on Image Processing*, 32:1927–1941, 2023. 2

[32] Xiangpeng Tian, Xiangyu Liao, Xiao Liu, Meng Li, and Chao Ren. Degradation-aware feature perturbation for all-in-one image restoration. In *Proceedings of the Computer Vision and Pattern Recognition Conference*, pages 28165–28175, 2025. 1, 3, 4, 7

[33] Yuchuan Tian, Jianhong Han, Hanting Chen, Yuanyuan Xi, Ning Ding, Jie Hu, Chao Xu, and Yunhe Wang. Instruct-ipt: All-in-one image processing transformer via weight modulation. *arXiv preprint arXiv:2407.00676*, 2024. 2

[34] Zhendong Wang, Xiaodong Cun, Jianmin Bao, Wengang Zhou, Jianzhuang Liu, and Houqiang Li. Uformer: A general u-shaped transformer for image restoration. In *Proceedings of the IEEE/CVF conference on computer vision and pattern recognition*, pages 17683–17693, 2022. 2

[35] Gang Wu, Junjun Jiang, Kui Jiang, Xianming Liu, and Liqiang Nie. Learning dynamic prompts for all-in-one image restoration. *IEEE Transactions on Image Processing*, 2025. 2

[36] Jie Xiao, Xueyang Fu, Aiping Liu, Feng Wu, and Zheng-Jun Zha. Image de-raining transformer. *IEEE transactions on pattern analysis and machine intelligence*, 45(11):12978–12995, 2022. 2

[37] Qihai Yan, Aiwen Jiang, Kang Chen, Long Peng, Qiaosi Yi, and Chunjie Zhang. Textual prompt guided image restoration. *Engineering Applications of Artificial Intelligence*, 155:110981, 2025. 1, 2

[38] Hao Yang, Liyuan Pan, Yan Yang, and Wei Liang. Language-driven all-in-one adverse weather removal. In *Proceedings of the IEEE/CVF conference on computer vision and pattern recognition*, pages 24902–24912, 2024. 1, 2

[39] Wenhan Yang, Robby T Tan, Jia Shi Feng, Jiaying Liu, Zongming Guo, and Shuicheng Yan. Deep joint rain detection and removal from a single image. In *Proceedings of the IEEE conference on computer vision and pattern recognition*, pages 1357–1366, 2017. 6

[40] Eduard Zamfir, Zongwei Wu, Nancy Mehta, Yuedong Tan, Danda Pani Paudel, Yulun Zhang, and Radu Timofte. Complexity experts are task-discriminative learners for any image restoration. In *Proceedings of the Computer Vision and Pattern Recognition Conference*, pages 12753–12763, 2025. 1, 3, 7

[41] Syed Waqas Zamir, Aditya Arora, Salman Khan, Munawar Hayat, Fahad Shahbaz Khan, Ming-Hsuan Yang, and Ling Shao. Multi-stage progressive image restoration. In *Proceedings of the IEEE/CVF conference on computer vision and pattern recognition*, pages 14821–14831, 2021. 2

[42] Syed Waqas Zamir, Aditya Arora, Salman Khan, Munawar Hayat, Fahad Shahbaz Khan, and Ming-Hsuan Yang. Restormer: Efficient transformer for high-resolution image restoration. In *Proceedings of the IEEE/CVF conference on computer vision and pattern recognition*, pages 5728–5739, 2022. 2, 3, 4, 7

[43] Haijin Zeng, Xiangming Wang, Yongyong Chen, Jingyong Su, and Jie Liu. Vision-language gradient descent-driven all-in-one deep unfolding networks. In *Proceedings of the Computer Vision and Pattern Recognition Conference*, pages 7524–7533, 2025. 7

[44] Rongyu Zhang, Yulin Luo, Jiaming Liu, Huanrui Yang, Zhen Dong, Denis Gudovskiy, Tomoyuki Okuno, Yohei Nakata, Kurt Keutzer, Yuan Du, et al. Efficient deweather mixture-of-experts with uncertainty-aware feature-wise linear modulation. In *Proceedings of the AAAI Conference on Artificial Intelligence*, pages 16812–16820, 2024. 1, 3

[45] Xu Zhang, Jiaqi Ma, Guoli Wang, Qian Zhang, Huan Zhang, and Lefei Zhang. Perceive-ir: Learning to perceive degradation better for all-in-one image restoration. *IEEE Transactions on Image Processing*, 2025. 2, 7

[46] Kaiwen Zhu, Jinjin Gu, Zhiyuan You, Yu Qiao, and Chao Dong. An intelligent agentic system for complex image restoration problems. In *The Thirteenth International Conference on Learning Representations*, 2025. 1, 3